A general combustion approach to multipod ZnO and its characterization

YU-NA ZHAO, MAO-SHENG CAO*, JIN-GANG LI
Department of Materials Science and Engineering, Beijing Institute of Technology, Beijing 100081, China
E-mail: caomaosheng@bit.edu.cn

YU-JIN CHEN
Institute of Physics, Chinese Academy of Sciences, Beijing 100081, China

Published online: 3 March 2006

By a general approach of combustion oxidation at high temperature, multipod ZnO was synthesized without any catalysts or additives. The morphology and optical properties of the multipod ZnO were studied in detail. The growth mechanism was discussed preliminarily. An ultraviolet (UV) emission peak at 374 nm and a broad green emission peak centered at 502 nm are observed in photoluminescence spectrum of the multipod ZnO. The multipod structure exhibits significant enhancement of UV emission intensity and green light emission intensity compared with the tetrapod structure, which are attributed to less structural defects and increased surface area respectively. Furthermore, compared with nano-particle and micro-particle ZnO, UV emission peak of multipod ZnO appears a slight blue shift. Due to slim tips of the legs, quantum size effect cause a slight blue shift of UV emission peak. We believe that these optical properties of the multipod structure have extensive applications in nanoscale optical devices.

1. Introduction

ZnO, as a wide band gap (3.37 eV) material with a large exciton binding energy (60 meV), is recognized as promising materials in many fields. ZnO has been attracted extensive attention due to its significant and fascinating applications in nanotechnology fields. It also has great potential for the fundamental studies of nanoscale chemistry and physics. Nanostructured ZnO may be one of the rich families due to diverse structures, whose configurations are much richer than any known nanomaterials including well-known carbon nanotubes. Up to date, using various techniques such as chemical vapor transport and condensation (CVTC) [1], thermal evaporation [2, 3], aqueous solution deposition [4], template-based growth [5], a wide range nanostructure ZnO have been synthesized, including nanowires [1, 6, 7], nanobelts [8], nanofilm [9, 10], nanorod [11–13], nanohelixes/nanosprings [14], nanotetrapod [2, 3]. These varied nanostructured ZnO exhibit many exceptional semiconducting, piezoelectric, and pyroelectric properties, etc. Moreover, they have been widely used in optoelectronics [15], nanosensor [16], nanoresonators [16], microwave absorbing materials [17] and biomedical science. ZnO nanostructure materials also gain much attention for optical applications [18]. Many characteristics of ZnO nanopowders are very sensitive to its surface state [19]. The multipod ZnO with a high surface to bulk ratio is expected to display remarkable properties in optical applications. At the present time, multipod ZnO nanostructure is synthesized by thermal evaporation method [4] and aqueous solution route [20–23]. In this paper, we report that multipod ZnO has been synthesized successfully by a simple combustion method without any catalysts, different completely from the traditional thermal evaporation method at high temperature. The morphology of the synthesized products is almost uniform, and the number of their legs is obviously more than four. The detailed analysis of its morphology is given, and the possible growth mechanism and the optical properties are discussed in detail.

2. Experimental procedure

The multipod ZnO was prepared via facile combustion oxidization approach without any catalysts, additives or

*Author to whom all correspondence should be addressed.

0022-2461
DOI: 10.1007/s10853-006-7176-5

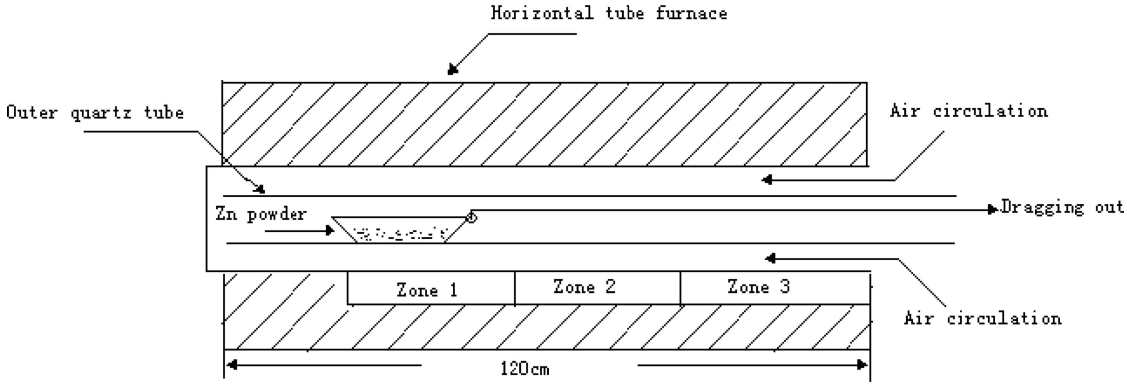

Figure 1 The schematic diagram of experimental apparatus for the growth of multipod ZnO.

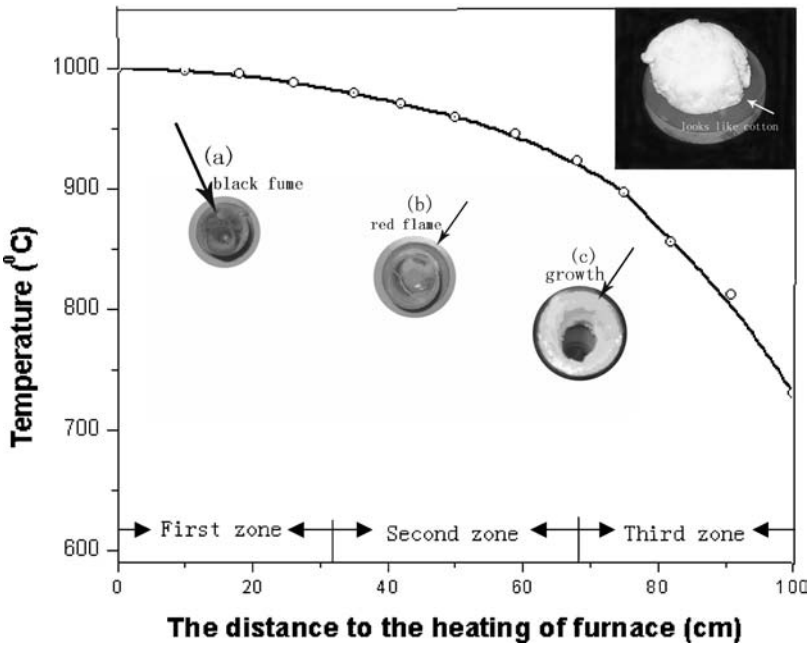

Figure 2 Temperature distribution diagram in the furnace, the insets show reaction phenomena in the different zones.

carrier gas at high temperature in open air. The schematic diagram of the experimental setup for the growth of multipod ZnO is shown in Fig. 1. Firstly, a larger fused quartz tube as outer tube, whose diameter is smaller than that of tube furnace, was inserted in a horizontal tube furnace with the length of 120 cm, the furnace temperature was ramped to about 800°C and kept at this temperature for half an hour. Then, a small fused quartz boat held with Zn powder (99.9%) was pushed in the larger tube. After the Zn powder was heated for about 1 min in the first zone, the black fume could be seen. 4 minutes later, the quartz boat was dragged out from the furnace slowly to the second zone. When the quartz boat was dragged out, the red flame was observed clearly. Then the boat was dragged out continuously, as a result, it can be seen clearly that the color of the product in the boat changed from yellow to white immediately in the third zone. Finally, the white product like cotton was obtained, as shown the upper inset in Fig. 2, the others insets show the reaction phenomena separately in the different zones. The morphology and size distribution of multipod ZnO had been examined by scanning electron microscopy (SEM, JSM-6301F), the microstructures were record in detail by transmission electron microscopy (TEM, JEM-2010F) operated at 200 keV. Photoluminescence (PL) spectra were measured by Xe light excitation source.

3. Result and discussion

The XRD pattern of the as-synthesized multipod ZnO is shown in Fig. 3, where the diffraction peaks of ZnO are sharp and narrow half width, the peaks of other impurity phase are not found. It also indicates that the microstructure of the product is typical hexagonal wurtzite structured ZnO with lattice parameters of a = 0.3249 nm and c = 0.5206 nm.

The SEM observations show clearly the general morphology of the multipod ZnO, as shown in Fig. 4. Fig. 4A reveals that the synthesized products consist of abundant multipod ZnO. Their morphology can be looked upon

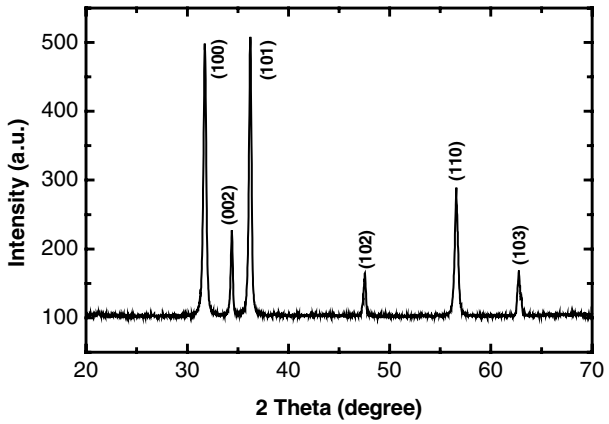

Figure 3 XRD pattern of the as-synthesized multipod ZnO.

as a central nucleus connecting with several legs with different length and number. Fig. 4C shows the single multipod ZnO with seven legs and a nucleus. Researchers consider widely that the formation of ZnO nanostructure has two stages: nucleation and growth. According to the octa-twin nucleus model [24], ZnO nuclei formed in the atmosphere containing oxygen are octa-twins nuclei which consist of eight tetrahedral-shape crystals, each consists of three $\{11\bar{2}2\}$ pyramidal facets and one (0001) basal facet. The eight tetrahedral crystals are connected together by making the pyramidal faces contact one with another to form an octahedron. Every twin is of the inversion type, the polarities of the twinned crystals are not mirror-symmetric with respect to the contacting plane but antisymmetric. Thus the eight basal surfaces of the octa-twins are alternately the plus surface $(0001)(+c)$ and the minus surface $(000\bar{1})(-c)$. In our experiments, Zn vapor began to react with oxygen at initial stage. Because the oxygen concentration was low at high temperature, ZnO initially formed was little and can be looked upon as central nuclei corresponding to octa-twins nuclei model. The energy dispersive X-ray spectroscopy (EDS) is shown in Fig. 4B, the peaks of other element are not found. During SEM characterization of mulitipod ZnO, Si slip was used as underlay, which led to peak of Si. Since no other elements exist, we may confirm that the central nuclei consist of ZnO formed initially. When the quartz boat was dragged out to the second zone, the air circulation forming between the outer quartz tube and boat supplied the oxygen for the coming growth, that is to say, the continuous growth from the eight facets happened. As a

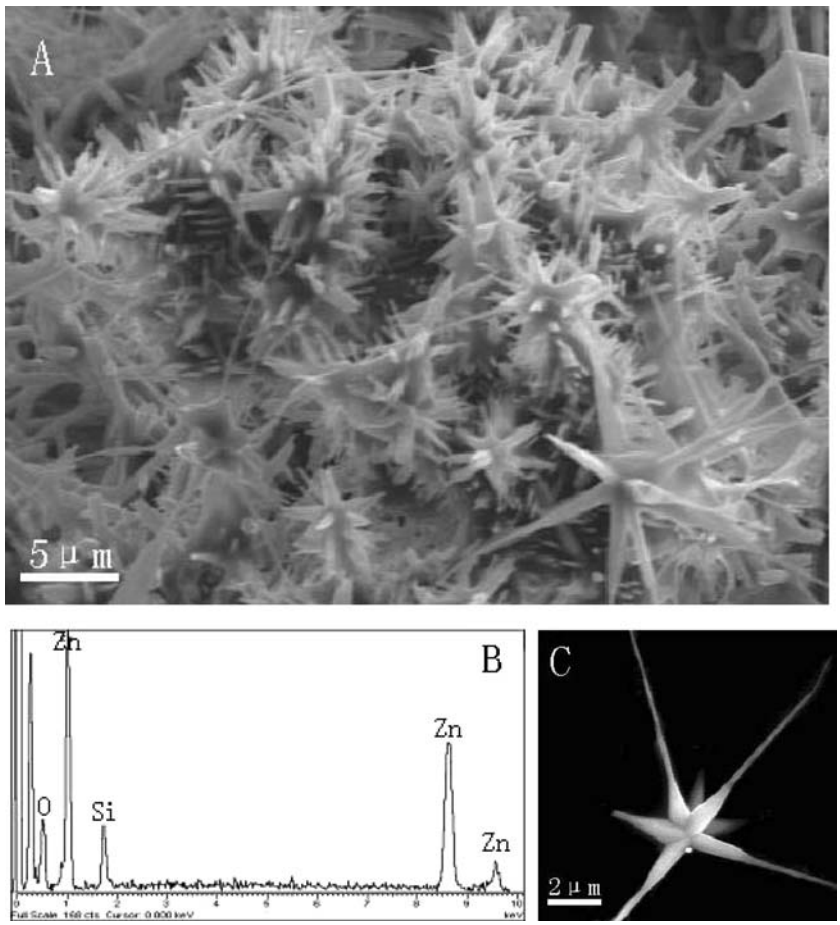

Figure 4 (A) shows the general SEM image of multipod ZnO structure. (B) EDS spectra from the multipod ZnO. (C) SEM image of the single multipod ZnO.

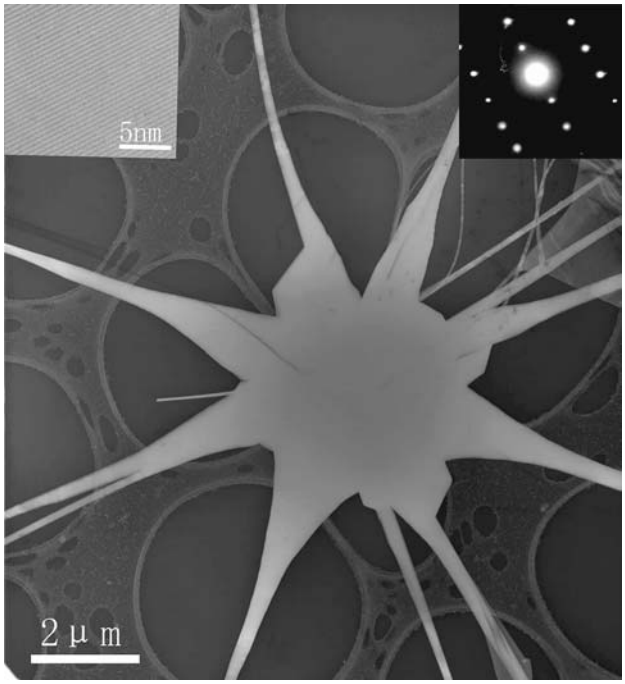

Figure 5 TEM image of the single multipod ZnO, the insets show the lattice fringe and the corresponding SEAD of one leg.

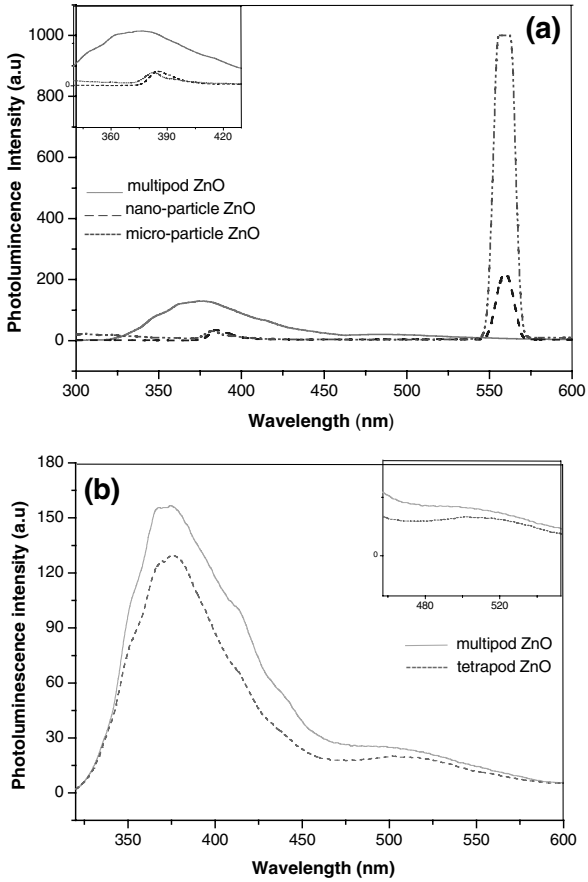

Figure 6 (a) represents PL spectrum comparison of multipod ZnO, nano-particle ZnO and micro-particle ZnO. The inset shows the amplificatory peaks of them around 374 nm. (b) indicates PL spectrum comparison of multipod ZnO and tetrapod ZnO. The inset shows the amplificatory peaks of them around 502 nm.

result, the eight legs should be formed around the central nucleus. On the other hand, it is well known that each octa-twins nucleus has four positively charged (0001) surfaces and four negatively charged (0001) surfaces [24]. The charged surfaces are likely to attract and react with Zn vapor and oxygen, resulting in the rapid growth of whiskers from eight facets, which further proves that multipod ZnO should have eight legs. However, different growth velocities along different facets could lead to different size of the legs, even some legs can not grow normally along the facets at all, so the SEM images in Fig. 4 show that the length and number of legs are not same. During the growth of the legs, the crystal could have stacking faults, not complete perfection. Furthermore, due to space restriction among the legs, the leg growing from some facets could be prevented, which results in that length and number of the legs growing from the same nucleus must not be identical.

To investigate the growth process of multipod ZnO structure in more detail, the further characterization was examined carefully by high-resolution TEM(HRTEM). Fig. 5 shows the TEM image of typical single multipod ZnO, which consists of eight legs and a central nucleus. It also indicates that the legs grow from the central nucleus along eight different directions, but the length and size of its legs is different, which demonstrate fully that the growth velocities of its legs are not same. The insets of Fig. 5 show the lattice fringes of one leg and the corresponding selected-area electron diffraction (SAED) patterns clearly, demonstrating that every leg of multipod ZnO structure is single crystalline. So the possible growth mechanism of multipod ZnO could be considered that the central nuclei are formed at initial reaction stage, and then its legs grow from the different facets of octa-twin central nucleus along the different directions. The growth of multipod ZnO by this simple method forms certain patterns and may enlighten more potential applications of ZnO in nanoscale devices.

PL spectra of mutipod ZnO were measured using Xe light (280 nm) as excitation source. Fig. 6(a) shows the PL spectra of multipod ZnO, compared with nano-particle ZnO and micro-particle ZnO separately. (Nano-particle and micro-particle are provided by Institute of Physics, Chinese Academy of Sciences). It can be observed that ultraviolet (UV) emission intensity of the multipod ZnO at room temperature increase obviously, and the peak position at ~374 nm appears a slight blue shift, whereas the UV emission peaks of nano-particle and micro-particle are at ~380 nm, the inset shows the amplificatory spectra of them around 374 nm. The UV emission can be explained by near band edge transition of wide band gap, namely the recombination of free excitons through an exciton-exciton collision process [25]. The quantum confinement effect related to the nanostructures is another

important factor responsible for the increase of the observed UV emission intensity at room temperature. Bagnall *et al*. [26] demonstrated that the improvement of crystal quality (decrease of impurities and structure defects) could result in detectable UV emission at room temperature. TEM image in Fig. 5 proves that multipod ZnO is with a low density of structural defects and the legs are single crystal structure, accounting for the strengthened intensity in the UV emission region. Due to the slim tips of the legs, the quantum size effect may be the reason that why the UV emission peak at 374 nm of multipod ZnO appears a slight blue shift. Such a phenomenon has been observed in nanowire with different diameter before [1]. Some changes can also be observed in the green emission region. The green emission region of multipod ZnO consists of a typical broad peak centered at 502 nm. However, no green emission peaks of nano-particle and micro-particle ZnO are found, the peaks at 560 nm of them are the peaks of frequency doubling from excitation source. The green emission peak is commonly referred to a deep-level or trap-state emission. Vanheusden *et al*. [27] have proved that the green transition attributes to the singly ionized oxygen vacancy in the ZnO and the emission results from the radiative recombination of a photogenerated hole with an electron occupying the oxygen vacancy. Therefore, it is reasonable to believe that the typical broad peak of multipod ZnO at 502 nm is caused by more ionized oxygen vacancies. Another possible reason for the broad peak may be that the morphology of the product is not identical. To research optical property of multipod ZnO in detail, another comparison with tetrapod (tetrapod ZnO is provided by Institute of Physics, Chinese Academy of Sciences [2]) is investigated, as shown in Fig. 6(b), UV emission peaks at ~374 nm are observed for them, the UV emission intensity of multipod ZnO is stronger obviously than tetrapod. In addition, the green emission peaks of them at ~502 nm are observed, but the green light emission intensity of multipod ZnO strengthens slightly, the inset shows the amplificatory spectra around 502 nm. According to above results, we can verify that UV light emission peak of multipod ZnO at 374 nm is attributed to the less structural defects than tetrapod ZnO. The enhanced green light emission intensity of multipod ZnO could be accounted for the increased surface area caused by more legs than that of tetrapod ZnO [23].

4. Conclusion

Multipod ZnO has been synthesized by a facile combustion oxidation approach without any catalysts and additives. The growth mechanism of multipod ZnO can be explained that the central nuclei are formed at initial stage, and then the legs grow respectively from the different facets of the octa-twin central nuclei. Room temperature PL spectrum of multipod ZnO can be attributed to the near band-edge emission and the deep-level green light emission. The multipod ZnO shows the strengthened UV emission peak, compared with nano-particle ZnO and micro-particle ZnO. In addition, UV emission peak of multipod ZnO appears a slight blue shift, which can be accounted for the quantum size effect. Furthermore, the more enhanced UV and green light emission intensity than tetrapod ZnO have been observed, which can be explained respectively by its less structural defects and larger surface area caused by more legs. Therefore we believe that multipod ZnO has many promising nanoscale applications in optoelectronics, light-emitting diodes, optical nanodevice and so on.

Acknowledgments

The authors thank national 863 (Grant No. 2002AA3 05509), 973 project (Grant No. 52318030301), National Natural Science Foundation (Grant No. 50572010) for providing the research grant.

References

1. M. H. HUANG, Y. WU, H. FEICK, N. TRAN, E. WEBER and P. YANG, *Adv. Mater.* **13** (2001) 113.
2. Q. WAN, K. YU and C. L. LIN, *Appl. Phys. Lett.* **83** (2003) 2253.
3. Z. CHEN, Z. W. SHAN, M. S. CAO, L. LU and S. X. MAO, *Nanotechnology* **15** (2004) 365.
4. Z. WANG, X. F. QIAN, J. YIN and Z. K. ZHU, *Langmuir.* **20** (2004) 3441.
5. Y. LI, G. W. MENG, L. D. ZHANG and F. PHILLIPP, *Appl. Phys. Lett* **76** (2000) 2011.
6. Y. C. KONG, D. P. YU, B. ZHANG, W. FENG and S. Q. FENG, *ibid.* **78** (2001) 407.
7. Y. W. WANG, L. D. ZHANG, G. Z. WANG, Z. Q. CHU and C. H. LIANG, *J. Cyst. Growth* **234** (2002) 171.
8. B. D. BAO, Y. F. CHEN and N. WANG, *Appl. Phys. Lett.* **81** (2002) 757.
9. S. H. KO. PARK and Y. EUILEE, *J. Mater. Sci.* **39** (2004) 2195.
10. H. S. LEE, J. Y. LEE, T. W. KIM, D. W. KIM and W. J. CHO, *ibid.* **39** (2004) 3525.
11. Y. DAI, Y. ZHANG, Q. K. LI and C. W. NAN, *Chem. Phys. Lett.* **358** (2002) 83.
12. C. XU, G. XU, Y. LIU and G. ZHANG, *Solid State Commun.* **122** (2002) 175.
13. L. GUO, J. X. CHENG, X. Y. LI, S. H. YANG, C. L. YANG and J. N. WANG, *Mater. Sci. Eng. C.* **16** (2001) 123.
14. R. YANG, Y. DING and Z. L. WANG, *Nano Lett.* **4** (2004) 1309.
15. B. P. ZHANG, N. T. BINH, H. WAKATSUKI, Y. KASHIWABA and K. HAGA, *Nanotechnology* **15** (2004) S382.
16. X. D. BAI, P. X. GAO and Z. L. WANG, *Appl. Phys. Lett.* **82** (2003) 4806.
17. Y. J. CHEN, M. S. CAO, T. H. WANG and Q. WAN, *ibid.* **84** (2004) 2415.
18. H. CAO, J. Y. XU, D. Z. ZHANG, S. H. CHANG, S. T. HO and E. W. SEELING, *Phys. Rev. Lett.* **84** (2000) 5584.
19. J. A. SCHWARZ and O. I. CONTESCU, *Surface of Nanoparticles and Porous Materials*, Marcel Dekker, New York, 1999.
20. A. B. DJUR, Y. H. LEUNG, W. C. H. CHOY, K. W. CHEAH and W. K. CHAN, *Appl. Phys. Lett.* **84** (2004) 2635.
21. X. SUN, X. CHEN and Y. D. LI. *J. Cyst. Growth.* **244** (2002) 218.
22. T. GAO, Y. HUANG and T. WANG, *J. Phys.: Condens. Matt.* **16** (2004) 1115.
23. Y. H. LEUNGA, A. B. DJURIS, W. C. H. CHOY, M. H. XIE, J. GAO, K. Y. K MAN and W. K. CHAN, *J. Cyst. Growth.* **274** (2005) 430.

24. S. TAKEUCHI, H. IWANAGA and M. FUJII, *Philos. Mag. A.* **69** (1994) 1125.
25. Y.C. KONG, D. P. YU, B. ZHANG, W. FANG and S. Q. FENG, *Appl. Phys. Lett.* **78** (2001) 407.
26. D. M. BAGNALL, Y. F. CHEN, M. Y. SHEN, Z. ZHU and T. YAO, *J. Cryst. Growth* **185** (1998) 605.
27. K. VANHEUSDEN, W. L. WARREN, C. H. SEAGER, D. K. TALLANT and B. E. GNADE, *J. Appl. Phys.* **79** (1996) 7983.

Received 21 April
and accepted 29 June 2005